Journal of Thermal Analysis and Calorimetry, Vol. 69 (2002) 785–794

CALORIMETRIC STUDIES OF THE ENERGY LANDSCAPES OF GLASSFORMERS BY HYPERQUENCHING METHODS

C. A. Angell[*]

Department of Chemistry and Biochemistryy, Arizona State University, Tempe, AZ85287-1604, USA

Abstract

We consider some of the conditions associated with ergodicity-breaking and vitrification, in particular the equivalent, in quench vitrification, of the $\omega\tau=1$ condition that is well-known in relaxation spectroscopy. For a given quench rate, $Q=dT/dt$, strong liquids are trapped at much higher temperatures, relative to T_g, than are fragile liquids. We relate the trapping of the system during quenches to the multidimensional 'energy landscape' by means of which the configurational microstates of the system are defined. To characterize the energy landscape at energy levels that are usually associated with fluid materials, we use differential scanning calorimetry on hyperquenched glasses. This yields not only the excess potential energies of the states trapped-in during quench Q, but also the trap depths. The latter are found to be much smaller, relative to kT_g, for strong liquids than they are for fragile liquids.

Keywords: energy landscape, fictive temperature, glass transition, hyperquenching

Introduction

The theoretical study of liquids has long been complicated by the problem of dealing with the entangled degrees of freedom that a liquid system explores at normal fluid temperatures. The existence of the supercooled liquid state, and of the glass transition that is manifested at lower temperatures by systems that are slow to crystallize, have made possible a major simplification in the theoretical handling of liquids. The simplification arises because of the possibility, in viscous liquids, of clearly separating the degrees of freedom that contribute to the liquid character. This separation depends on the development, on supercooling, of a great difference in the time scales on which the particles of the system vibrate, on the one hand, and migrate, on the other. This short article is devoted to showing how calorimetry can contribute to the understanding and characterization of the degrees of freedom involved in migration and, more broadly, in the determination of the 'structural energetics' of a liquid.

* E-mail: caa@asu.edu

1418–2874/2002/ $ 5.00

Akadémiai Kiadó, Budapest
Kluwer Academic Publishers, Dordrecht

The vibrational degrees of freedom of a glass, like those of a crystal, can be described in terms of elementary vibrational degrees of freedom, or phonons. In crystals these 'elementary excitations' have a simple character such that for a given branch of the phonon spectrum there is a unique relation between phonon wavelength and phonon frequency (hence energy). In glasses, due to their disorder, the relation is more complex, and distribution functions must be invoked, but still the notion of elementary vibrational excitations remains valid.

At temperatures above the 'glass transition temperature', the system begins to explore a new degree of freedom, which involves the change of structure of the system within which the phonons are excited. This glass transition temperature seems to occur when the vibrational amplitude reaches a critical value, as in the Lindemann criterion for the melting of crystals [1–4]. The temperature at which the exploration of the new degree of freedom commences, called the 'glass transition temperature', depends on the time scale on which the system's temperature is raised. Inversely, and more appropriately for this article, the temperature at which the exploration of this degree of freedom ceases, is determined by the cooling rate. We are interested in the trapping of the system at high temperatures by very rapid cooling, and the determination of the energetics of the trapped-in state by low scan rate calorimetric study. First we discuss the phenomenology of trapping.

Vitrification

Consider the ability of a system of dipoles to 'follow' (remain in phase with) a fluctuating electric field of frequency ω. It is determined by the relation between the 'dielectric relaxation time' of the system τ and the field frequency ω. The system follows the field so long as ω, the angular frequency of the field, is well below the value $2\pi/\tau$. When the field frequency is much higher than the value $2\pi/\tau$, the dipolar system is essentially frozen and the dielectric constant measured in the experiment has its glassy value, i.e. ergodicity has been broken. The crossover between ergodic and non-ergodic behavior can be thought of as occurring when the condition

$$\omega\tau=1 \tag{1}$$

is met [5]. This is the condition for which the dielectric loss spectrum ε'' *vs*. log frequency, has its maximum value, and energy is dissipated from the field at a maximum rate [6].

In the same way, the ability of a system of mobile particles to remain in equilibrium during cooling at a given quench rate dT/dt is determined by the relaxation time, except that now it is the temperature dependence of the relaxation time that is important, and it is the hysteresis spectrum that has a maximum value. The hysteresis spectrum [7, 8] is determined by the difference between the values of some extensive property, or any other structurally sensitive indicator (such as an optical absorption intensity [8] when measured during cooling on the one hand and during heating at the same rate, on the other. Examples are given below.

In analogy to Eq. (1), the maximum in the hysteresis spectrum of a viscous liquid observed, during cooling *vs*. heating at the rate $\pm Q/$ K s^{-1}, is reached when the condition

$$dT/dt\,d\tau/dT=1$$

$$\text{i.e. } Q\,d\tau/dT=1, \tag{2}$$

is satisfied. Equation (2) has been discussed for the case of structure freezing in computer simulation studies in which Q is extremely high, and $d\tau/dT$ accordingly very low, when ergodicity is broken. In particular Eq. (2) has been discussed by Cooper and co-workers [9] who called it the Lillie number.

We depict this phenomenology in Fig. 1, using volume as the extensive variable whose variation with temperature during cooling is compared with the temperature dependence of the relaxation time and Fig. 2, using enthalpy and optical absorption. The hysteresis, in both enthalpy and in optical absorptivity of a structural probe species, is shown in Fig. 2 panel (a). The derivatives of the heating scans which are usually used to determine T_g are shown in Fig. 2 panel (b) and the hysteresis spectra are shown in Fig. 2 panel (c). Note that the maxima in the hysteresis spectra occur at essentially the 'onset T_g' which is also where the fictive temperature [10] (i.e. trapping temperature), is found to lie [10, 11], Fig. 3, panel (a).

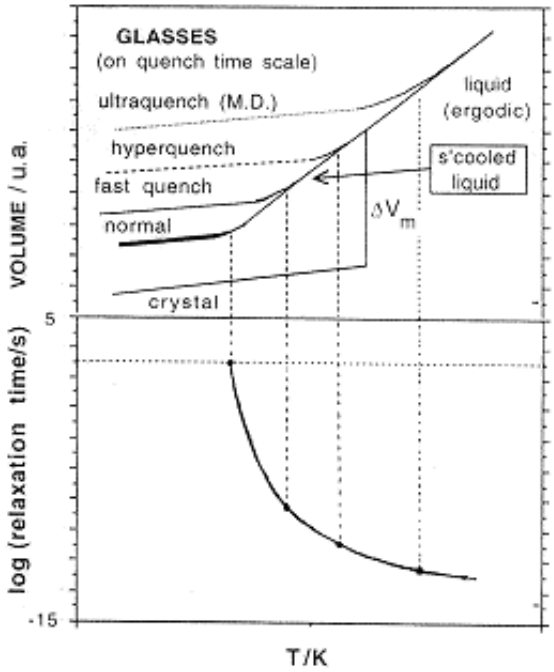

Fig. 1 Schematic showing the course of the liquid volume during cooling at different quench rates, $-Q$/K min^{-1}. Lower panel shows the relation of the temperature of arrest during cooling to the temperature dependence of the relaxation time, in accord with Eq. (2)

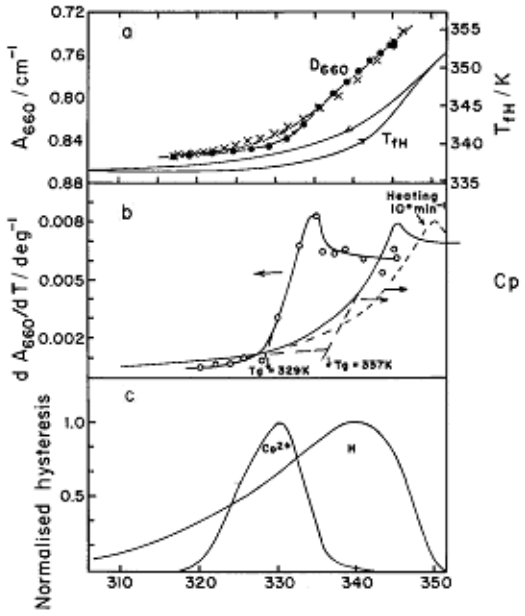

Fig. 2 Examples of the hysteresis of enthalpy, and optical absorption of probe Co(II) ions, through the glass transformation range of CKN ($40Ca(NO_3)_2{\cdot}60KNO_3$) (panel (a), showing the derivatives which are normally used to define the glass transition panel (b), and (lower panel) the hysteresis spectra obtained from panel (a). The maximum in the hysteresis spectrum corresponds closely with the onset glass transition temperature, and with the fictive temperature as defined by Moynihan *et al*. [10] (also [11]) (from Wong and Angell, [7])

A quantity which corresponds to the LHS of Eq. (2) is often discussed in glass science text books where it is called the Deborah Number, dt/dτ (Structural Chemistry of Glasses by Rao, Elsevier Science). It is usually observed that for ordinary cooling rates, the temperature dependence of relaxation times dτ/dT is such that the *DN* (written out in Eq. (2) form as Qdτ/dT) has the value unity. What is not usually observed is that the *DN* must have the value unity irrespective of cooling rate because *DN*=1 defines the condition for ergodicity breaking. A detailed quantitative assessment of this relationship has yet to be reported for glasses formed at very different quenching rates.

We can exploit Eq. (2) in the context of the variable fragility of glassformers to make some predictions about quench rate/fictive temperature relations. Reflecting Eq. (2), Fig. 1 shows that the temperature of trapping will be highest when the temperature dependence of relaxation is lowest. For a strong liquid, in which the relaxation time temperature dependence is low at all temperatures relative to T_g, [3], a very large range of trapping temperatures should be open for exploration even with the use of a modest range of quenching rates. For fragile liquids, in which the temperature de-

pendence of the relaxation time is very large near T_g, a much smaller range of temperatures will be sampled with the same range of quenching rates.

Most interesting from the point of view of new understanding of the liquid state will be the manner in which the equilibrium state is recovered as the trapped-in state is reheated.

This is because of the manner in which the trapped-in energy and the recovery of the equilibrium state is related to the 'energy landscape' by means of which the structural microstates of the liquid system are currently being interpreted and quantified. We discuss this in the next section.

Energy landscape interpretation

A vitrified liquid, according to Goldstein [12] and Stillinger and Weber [13], is to be viewed as a single system point trapped in a local minimum of potential energy [11], or 'basin of attraction' [12], on a $3N+1$ dimensional hypersurface (or 'energy landscape') for that system. This potential energy hypersurface is uniquely determined by the Cartesian coordinates of the N particles of the system (avoiding repulsive overlays), on the one hand, and the potential energy of interaction between these particles, on the other. These basins are the configurational microstates of the system in terms of which the structural component of the system's free energy is to be described. Elsewhere they have been called 'configurons' [14]. The configurational entropy of a liquid is determined by the number of configurons N_c accessible to it at the temperature in question, $S_c=k_B\ln W=k_B\ln N_c(T)$. Since the total number W of distinct packing states available to a system of N particles is found to increase as some exponential function of N, $W=\exp(\alpha N)$ where α is close to unity [15], the total configurational entropy is about $k_B N_{Avogadro}$ per mole of atoms (or R entropy units per mole of rearrangeable subunits, in the case of molecules). A proper understanding of the configurational aspect of the liquid thermodynamics therefore depends on the develop-

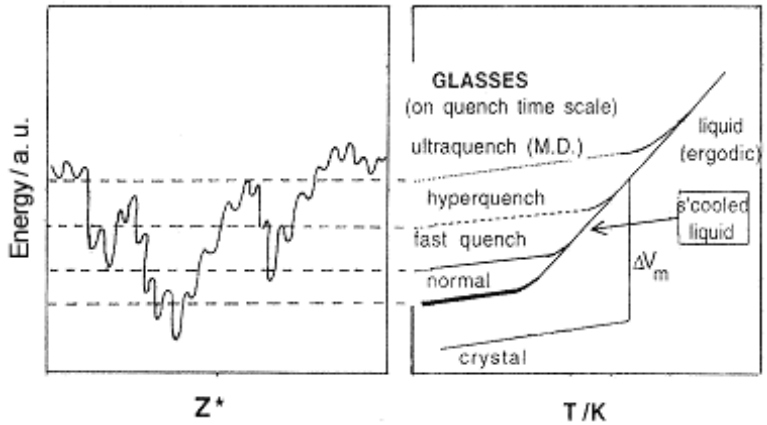

Fig. 3 Depiction of the relation between the landscape energy of the basin in which the system is trapped during quenching and the rate of the

ment of an appropriate quantification of the topology of the potential energy hypersurface.

The process of maintaining equilibrium, or approaching equilibrium, involves the exploration of the potential 'energy landscape'. The system point must move between a large enough subset of the basins at the appropriate level on the landscape to effectively have explored them all. To achieve the equipartition of kinetic and potential energy that determines a state of equilibrium, the degrees of freedom involved must communicate. There must be an exchange of energy between the phonon and configuron microstates of the system. Clearly, at equilibrium, the forward and reverse exchange rates between these microstates must be the same. Otherwise the system is said to be annealing, and its properties are time-dependent. When the phonon-configuron exchange which is responsible for maintaining equilibrium, becomes too slow, then equipartition fails, and the system becomes non-ergodic as in glass formation.

The energy of the basin in which the system becomes trapped during continuous cooling is higher the higher the cooling rate. The energy is like the volume depicted in Fig. 1 though is not as simple to visualize. The energy of the trapped state can be depicted for different cooling rates as in Fig. 3. What is of interest to discover, from the point of view of improved understanding of the energy hypersurface, is not only energy of the trapped state for a given cooling rate, but also the depth of the basin in which the system is trapped in relation to the energy of the basin.

Calorimetric quantification of energy landscape characteristics

Both of the latter characteristics of the trapped ('glassy') state can be determined calorimetrically, by studies made subsequent to the initial trapping. The energy difference between quenched glass and 'standard' glass can be assessed by comparison of the differential scanning calorimetry upscans, at constant scan rate, after cooling at the standard rate on the one hand and at the higher rate $-Q$ of the quench, on the other. We reproduce an example from a recent paper on this subject [11], in Fig. 4.

Panel (a) of Fig. 4 shows the standard and non-standard upscans both conducted at the upscan rate of 20 K min^{-1}. Panel (b) shows the difference in area between the standard and quenched samples. The integral under the panel (b) difference plots (or over them in the case of cooling rates slower than the standard rate) of this difference gives the difference in energy between the standard glass and the quenched glass. The dashed line is the value for a hyperquenched glass, cooled at an estimated 10^6 K min^{-1} [10]. The integral, or energy difference, in this case is of course large because the system was trapped high up on its energy landscape. The temperature of trapping, or fictive temperature, can be determined by the construction shown in [9] and [10] and compared with the value predicted from the relaxation time temperature dependence, according to Eq. (2), if the quenching rate is known from other measurements. For the hyperquenched OTP shown in Fig. 3(b), the fictive temperature was estimated to be 1.076 T_g, corresponding to a quench rate of about 10^5 K s^{-1}. Much

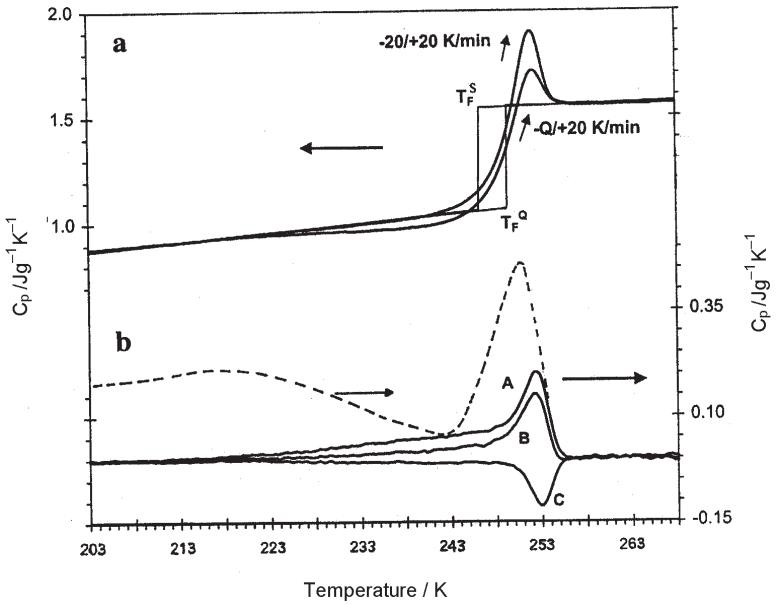

Fig. 4 a – DSC upscans at the ('standard') heating rate, $+Q^S$) of 20 K min^{-1}, of two *o*-terphenyl OTP glasses formed at different cooling rates, (i) –20 K min^{-1}, ($-Q^S$) and (ii) a rate, $-Q$/K min^{-1} (–247 K min^{-1}). The upper scan is called the 'standard scan'. Step function defines fictive temperature of the standard scan, which is seen to coincide with the glass transition temperature defined by the 'C_p onset' criterion, as mentioned earlier. The area between the scans is used to obtain the fictive temperature of the faster-cooled glass, T_F^Q
b – Excess heat capacities for non-standard scans (right hand ordinate, solid curves): The difference between the two curves of part (a) is shown as curve A. All heating rates are 20 K min^{-1}. Curve B is for a cooling rate of –73 K, and curve C is for 10 K min^{-1} cooling. Their integrals are used to obtain the fictive temperatures [10, 11], referred to the fictive temperature of the standard scan. The dashed curve is the excess heat capacity obtained for the hyperquenched OTP sample, which was quenched at a rate some four orders of magnitude faster than any of the others (see text), hence exhibits a much greater excess heat capacity (for complete exotherm, Fig. 4). The excess heat capacity for hyperquenched glasses is also of different form, showing a maximum well below T_g (from [11], by permission)

higher relative fictive temperatures are estimated for stronger liquids quenched at comparable rates [19, 20].

The depth of the basin in which the system was trapped can be estimated from the temperature at which the trapped-in enthalpy starts to be released during the rescan.

Assigning an attempt frequency ω_0 of 10^{13} Hz, the system will start to release heat when its enthalpy relaxation time reaches 100–200 s for an upscan at 20 K min^{-1}. This is because 100–200 s is the internal (sample) time scale that must cross the experimental time scale (determined by the scan rate) in order for 'ergodicity to be restored', i.e to start recovery of the equilibrium state. The energy of the barrier oppos-

ing the relaxation can then be obtained from the Boltzmann probability, per attempt, of escaping from the trap at the temperature T_{esc}, viz.,

$$P_{(escape)}=\exp(-E_{trap}/RT) \quad (3)$$

Equating 100 s to the product of time per attempt [$\tau_0=(2\pi\omega_0)^{-1}$] and probability of escape, we obtain

$$100=10^{-14}\exp(E_{trap}/RT),$$

from which

$$E_{trap} = 2.303\, RT_{esc} \log 10^{16}=36.8\, RT_{esc} \quad (4)$$

where T_{esc} is the temperature at which the enthalpy recovery commences during the upscan.

Evidently, the depth of the 'basins' occupied by the system will vary with time during the annealing as the system moves to lower and lower levels on the energy landscape. Thus we arrive at a picture of a landscape with fewer and fewer minima, of greater and greater depths, as lower and lower energies are explored. Whether these deeper minima are associated with higher densities or not will depend on the system under study. In some systems, such as water, the energy is inversely proportional to volume mass. The relation between the basins explored during the annealing of hyperquenched liquids, such as are discussed herein, and the glasses produced by vapor deposition and explored in considerable detail by Fujimori and Oguni [21] with respect to annealing kinetics, is not clear at this time. It is a matter of much interest. This study, and the more recent study of

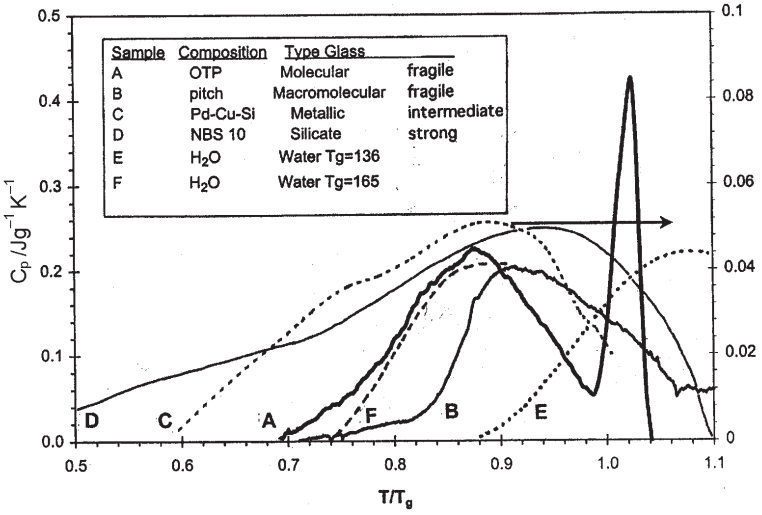

Fig. 5 Excess heat capacities of hyperquenched glassy solids exhibited during rescan from low temperatures, showing the release of the trapped-in energy and revealing aspects of the energy landscape not available from other studies. Systems are of different fragilities as indicated in the legend. Details are available in [11] (from [11], by permission)

hyperquenched basalt glass, using anneal-and-scan methods, by Yue and co-workers [19] indicate the wealth of information available from hyperquenched glass studies. A complication is that, in view of the existence of a distribution of structural relaxation times for glasses, there can be no unique fictive temperature assigned to a given glass, only some average value. The experimental manifestations of this complication will be discussed in a future article [22].

Some data for the excess heat capacity of hyperquenched glasses, formed from liquids of different fragility, are shown in Fig. 4. Quench rates were all in the range 10^5–10^6 ks^{-1}. Figure 5 shows that for the strongest liquids, the trapped-in enthalpy starts to be released at very low temperature relative to T_g, while for the more fragile liquids, the release only commences quite close to T_g. Qualitatively, the relation is the same as for the width of the glass transition, which is very broad for strong liquids and narrow for fragile liquids [16–18].

It is desirable that a combination of computer simulation experiments, hyperquenching experiments and long time annealing experiments, be conducted on model systems of different fragilities, in which the potentials available give good agreement with experiment, as with BeF_2 [23, 24] and to a lesser extent SiO_2 [25, 26]. Such studies may be expected to reveal detailed quantitative information on the structure of the energy landscape for such systems, and thus to facilitate the full description of the energetics, and related dynamic features, of glassforming liquids.

* * *

This work was supported by the National Science Foundation under Solid State Chemistry grant No. DMR –0082535.

References

1 U. Buchenau and R. Zorn, Europhys. Lett., 18 (1992) 523.
2 C. A. Angell, Science, 267 (1995) 1924.
3 X. Xia and P. G. Wolynes, Proc. Nat. Acad. Sci., 97 (2000) 2990.
4 C. A. Angell, J. Amer. Ceram. Soc., 51 (1968) 117.
5 C. P. Smyth, Dielectric Behavior and Structure, McGraw Hill, New York 1955, p. 431.
6 T. Matsuo, H. Suga and S. Seki, Bull. Chem. Soc., Japan, 39 (1966) 1827.
7 J. Wong and C. A. Angell, Glass: Structure by Spectroscopy, Marcel Dekker, New York 1976.
8 A. Barkatt and C. A. Angell, J. Chem. Phys., 70 (1979) 901.
9 a) A. R. Cooper and P. K. Gupta, Phys. and Chem. of Glasses 23 (1982) 44.
b) A. R. Cooper, J. Non-Cryst. Solids, 71 (1985) 5.
c) O. V. Mazurin and A. R. Cooper, JNCS, 72 (1985) 65.
10 M. A. DeBolt, A. J. Easteal, J. Wilder and J. Tucker, J. Phys. Chem., 78 (1974) 2673.
11 a) V. Velikov, S. Borick and C. A. Angell, J. Phys. Chem., 106 (2002) 1069.
b) Science, 294 (2001) 2335.
12 M. Goldstein, J. Chem. Phys., 51 (1969) 3728.
13 F. H. Stillinger and T. A. Weber, Science, 228 (1984) 983.
14 a) C. A. Angell, J. Am. Ceram. Soc., 51 (1968) 117;
b) C. A. Angell, J. Phys. Cond. Matter, 12 (2000) 6463.

15 R. J. Speedy, J. Phys. Chem., 103 (1999) 4060.
16 J. Lucas, Hong Li Ma, X. H. Zhang, H. Senapati, R. Böhmer and C. A. Angell, J. Sol. State Chem., 96 (1992) 181.
17 C. T. Moynihan, J. Am. Ceram. Soc., 76 (1993) 1081.
18 K. Ito, C. T. Moynihan and C. A. Angell, Nature, 398 (1999) 492.
19 a) Y. Yue, Proc. Edinburgh Internat. Congress on Glass, 2001, p. 833;
b) Y.-Z. Yue, J. deC. Christiansen and S. L. Jensen, Chem. Phys. Lett., 20 (2002) 357.
20 J. Huang and P. Gupta, J. Non-Crystalline Solids, 151 (1992) 175.
21 H. Fujimori and M. Oguni, J. Chem. Thermodyn., 26 (1994) 367.
22 C. A. Angell, Y.–Z. Yue, L.-M. Wang, J. R. D. Copley and S. Borick: http://www.df.unipi.it/workshop/workshop.html
23 M. Hemmati, C. T. Moynihan and A. Angell, J. Chem. Phys., 5 (2001) 6663.
24 M. Wilson and P. A. Maden, J. Phys. Condensed Matter, 6 (1994) A151; 5 (1993) 6833.
25 J. Horbach, W. Kob and K. Binder, Phil. Mag., B, 77 (1988) 297.
26 M. Hemmati and C. A. Angell, 'Physics meets Mineralogy', Eds H. Aoki and R. Hemley, Cambridge Univ. Press Chap. 6.1, pp. 325.